Case Studies in Construction Materials 11 (2019) e00252

Contents lists available at ScienceDirect

Case Studies in Construction Materials

journal homepage: www.elsevier.com/locate/cscm

Short Communication

The architrave *a tasselli*

Angelo Aloisio*, Rocco Alaggio, Massimo Fragiacomo

Department of Civil, Construction-Architectural and Environmental Engineering, Università degli Studi dell'Aquila, Via G. Gronchi, 18, L'Aquila, 67100 Abruzzo, Italy

ARTICLE INFO

Article history:
Received 21 February 2019
Received in revised form 13 May 2019
Accepted 15 May 2019

Keywords:
Architectural heritage
Theory of elasticity
Masonry building
Traditional constructive techniques

ABSTRACT

The architrave a *tasselli* is a peculiar design shape of the traditional stone lintels, which are widespread in Abruzzo, Italy: stone lintels are not usually monolithic elements, being formed by three pieces, the block spanning the opening and the *tasselli*, two small rectangular pieces. In the current paper, by means of an elementary Wrinkler-type beam model, it has been attempted to capture the behaviour of stone lintels, chasing the mechanical reasons supporting this traditional construction technique.

1. Introduction

The use of stone architraves belongs to the architectural heritage of many traditional buildings in Abruzzo, Italy. Their use is now confined to restoration works, since masonry is considered obsolete for new buildings.

The architraves, which are widespread in Abruzzo (Italy), have two main configurations, Fig. 1: a standard one, i.e. a monolithic element spanning from one support to the other and the so-called *a tasselli* configuration.

Varagnoli [1,2] was the first to introduce such nomenclature *a tasselli*, to intend the disarticulation of stone lintels into three parts: a central one, resting on the piers, roughly for one third of their sections, and two extreme pieces the *tasselli*.

In this paper, the authors will refer to the architave *a tasselli* as to the Piece-Type (PT) architrave. It may be difficult to understand why the architraves, belonging to the second configuration, are widespread in earthquake-prone areas [3–6,21]: an adequate toothing of the architraves inside the masonry should be an important requirement for spandrels-piers frame interaction under earthquake [7–9].

Actually, hundreds of examples of similar architraves can be found in Abruzzo, Fig. 2. The use of the PT architraves is a technique difficult to date, many examples are evidenced from mid-1700s buildings, up to the early 1900s, Fig. 2 [10–12]. In this paper an elementary mathematical model representing the PT architrave is proposed, then it is attempted to understand the physical reasons supporting the peculiar disarticulation of stone lintels into three sub-elements.

* Corresponding author.
E-mail addresses: angelo.aloisio1@graduate.univaq.it (A. Aloisio), rocco.alaggio@ing.univaq.it (R. Alaggio), massimo.fragiacomo@univaq.it (M. Fragiacomo).

https://doi.org/10.1016/j.cscm.2019.e00252

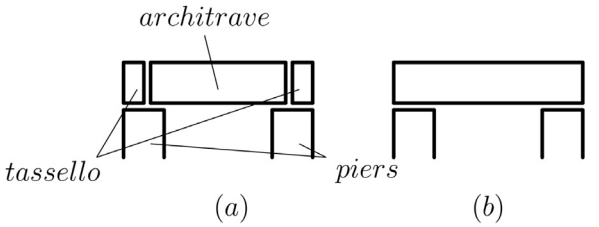

Fig. 1. The main geometric configurations of architraves in Abruzzo, (a) an architrave *a tasselli*, (b) a monolithic architrave.

2. Methods and mathematical model

An 2-D elementary analytical model of the architrave standing on its piers is proposed, Fig. 3. The block spanning the opening is treated as an Euler–Bernoulli-type beam [14,16], while the two portions standing on the piers as Winkler-type beams [13,15].

The choice of the c coefficient, Winkler's constant, expressing the subgrade's stiffness [17,18], is the key of the current paper: c depends on the interaction between stone and stone, architrave and piers, that is between two homogeneous surfaces (Fig. 4).

Many factors may concur to the definition of an equivalent elastic constant: from the surface roughness, to the quantity and quality of the mortar between lintel and piers, to the elastic properties of stone, to three-dimensional effects, not to mention load-histories dependencies and other factors difficult to confine within the theory of elasticity. In Eq. (1), the considered factors are resumed:

$$c = f(E_s, E_m, s, \rho_s, D_3, e) \tag{1}$$

E_s, Young modulus of the stone; E_m, Young modulus of the mortar; s, equivalent thickness of the surface roughness; ρ_s, equivalent density of the surface roughness; D_3, 3-D effects; e, other factors.

Given the complexity in the definition of c, its estimate may derive from rough dimensional considerations: if the elastic subgrade, which c represents, is a layer with thickness s and modulus of elasticity E, its stiffness is E/s. c is, in fact, a force $[F]$ over a length's cube $[F/L^3]$, so the estimation of c may be achieved by dividing the Young modulus E for an equivalent length s, Eq. (2).

$$c = \frac{E}{s} \tag{2}$$

E, Young modulus; s, equivalent thickness.

The elastic interaction between piers and lintels may be synthetically expressed by an equivalent layer, corresponding to the roughness of the two facing surfaces: E identifies the modulus of elasticity of the surface roughness, while s the corresponding equivalent thickness. The roughness between piers and lintels may act, in fact, like uniformly distributed elastic springs. The stone aggregates too, belonging to the thin mortar layer between lintel and pier, may behave like a uniform elastic medium characterized by its mean thickness and the Young modulus ($E_s = E$[1] Eq. (2)) of the aggregates.

The physical meaning of c is so founded on the roughness of the facing surfaces of lintels and piers. A parametric analysis is now carried out, assuming different values of s. From Eq. (2), assuming the Young modulus of the beam E_s equal to that of c in Eq. (2), the equivalent lenght of the Winkler-type beam [14] depends on the sole inertia I and the s parameter.

$$\lambda = 2\pi \left[\frac{EI}{c}\right]^{1/4} = 2\pi [Is]^{1/4} \tag{3}$$

λ, characteristic length of Winkler equation; I, cross section inertia.

The elastic problem is summarized in Table 1, listing for each beam portion, according to notation in Fig. 3, the corresponding differential equations as well as the respective boundary conditions in terms of the displacement variable v.

Noteworthy, given the same s H (lintel span) and L (lintel height), the results are not load-dependent, see Eq. (4) and (5).

$$\begin{cases} \phi(x) = v'(x) \\ T(x) = -EIv'''(x) \\ M(x) = EIv''(x) \end{cases} \tag{4}$$

[1] $E_s = E_{stone}$ is the beam Young modulus, while E is the one defined in Eq. (2).

Fig. 2. Examples of the PT architrave. The red lines highlight the dis-articulation of the architrave into three elements, the block spanning the opening and the two lateral pieces.

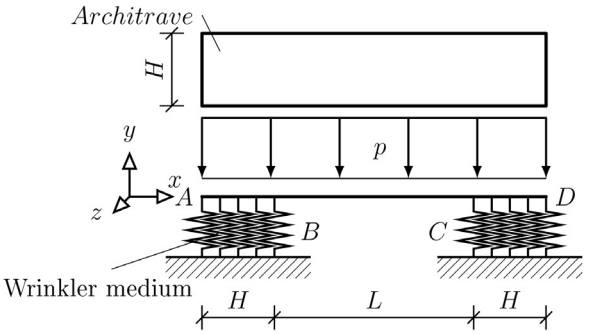

Fig. 3. Structural sketch of the PT architrave.

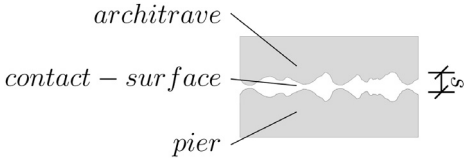

Fig. 4. Enlarged scheme of the contact surfaces of piers and architrave.

Table 1
Description of the mathematical model of the PT architrave.

A–B		$EIv_1^{IV}(x) + p = 0$ $v_1(x)$=vertical displacement x= beam's axis abscissa E=Young's modulus I=Section's inertia p=vertical load c=Winkler constant	$v_1''(A) = 0$ $v_1'''(A) = 0$
B-C	Bernoulli equation	$EIv_2^{IV}(x) + p = 0$ $v_2(x)$=vertical displacement E=Young's modulus I=Section's inertia p=vertical load c=Winkler constant	$v_1(B) = v_2(B)$ $v_1'(B) = v_2'(B)$ $v_1''(B) = v_2''(B)$ $v_1'''(B) = v_2'''(B)$ $v_2(C) = v_3(C)$ $v_2'(C) = v_3'(C)$ $v_3''(C) = v_3''(C)$ $v_2'''(C) = v_2'''(C)$
C–D	Winkler equation	$EIv_3^{IV}(x) + p = 0$ $v_3(x)$=vertical displacement E=Young's modulus I=Section's inertia p=vertical load c= Winkler constant	$v_3''(D) = 0$ $v_3'''(D) = 0$

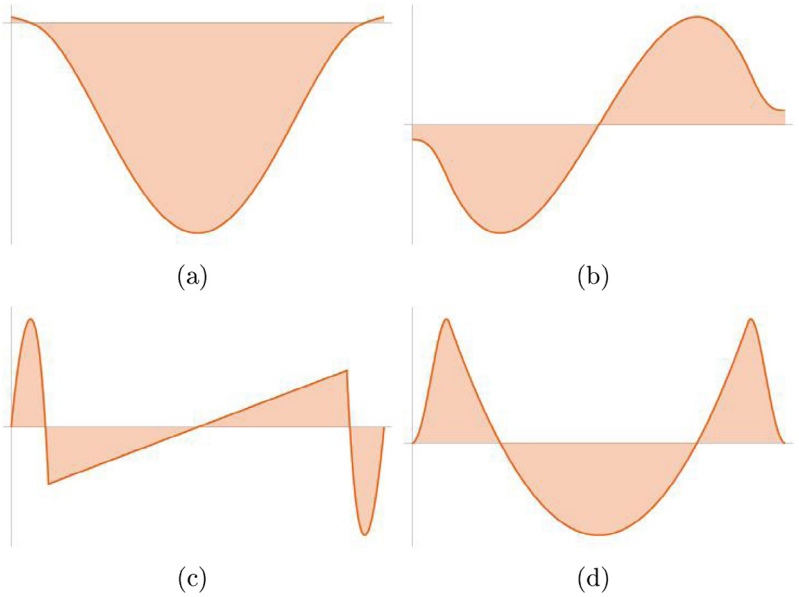

Fig. 5. Qualitative trend of the solution of equations in Table 1, in particular (a) the displacement (b) the rotation (c) the shear and (d) the bending moment.

$\phi(x)$, rotation of the beam cross section; $T(x)$, shear; $M(x)$, bending moment.

$$\left[\frac{v(x)}{p}, \frac{\phi(x)}{p}, \frac{T(x)}{p}, \frac{M(x)}{p}\right] = f(s, L, H) \tag{5}$$

s, equivalent thickness of the surface roughness; L, Lintel span; H, Lintel height.

The three variables s,H and L are used to perform a parametric analysis in Eq. (5).

In Fig. 5, the general trend of the results terms of displacement (Fig. 5(a)), section rotation (Fig. 5(b)), shear (Fig. 5(c)) and bending moment (Fig. 5(d)) is shown.

Since the bending moment depends on the s, L and H variables, different ratios k, between maximum and minimum bending moment (M_{max} and M_{min} respectively), are estimated, Eq. (6) and Fig. 6.

$$k = \frac{|M_{\min}|}{M_{\max}} \tag{6}$$

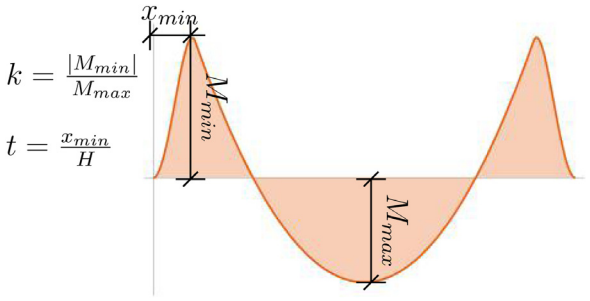

Fig. 6. Graphical representation of the variables involved in the parametric analysis.

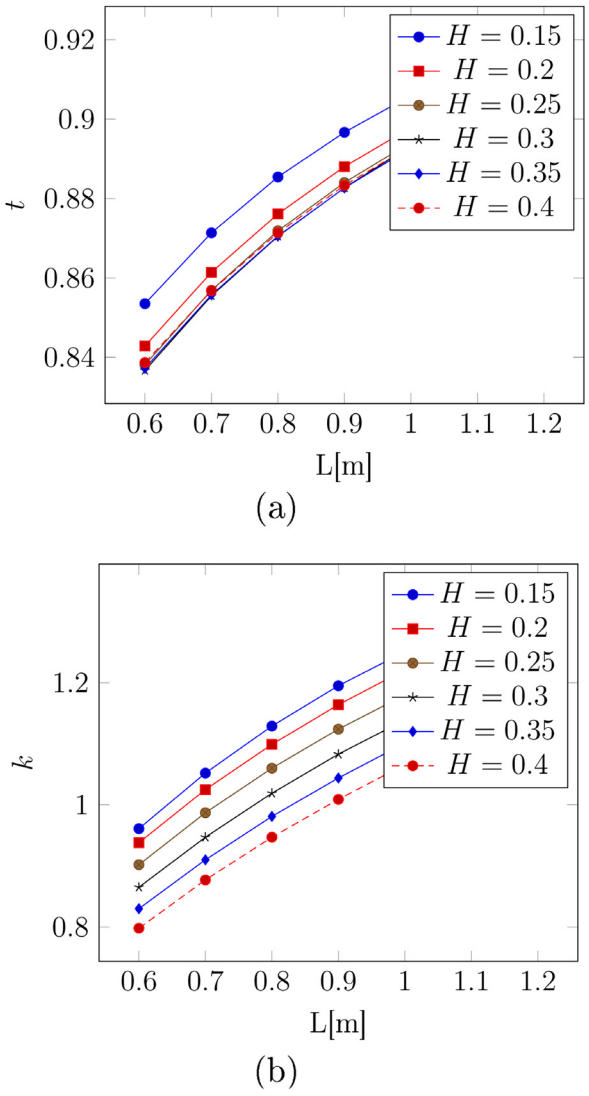

Fig. 7. Parametric analysis of the $t(L)$ (a) and $k(L)$ (b) functions for 6 different values of H, assuming $s = 5$ mm.

k, bending moment ratio; M_{max}, maximum bending moment in the $(B - C)$ beam portion; M_{min}, minimum bending moment over the beam supports $(A - B)$ and $(C - D)$.

The position x_{min} of M_{min} depends on the same s, L and H parameters, Fig. 6.

The ratio, t, Eq. (7) between the position of the minimum bending moment with respect to point A and the width of the supports is so defined, Fig. 6:

$$t = \frac{x_{\min}}{H} \tag{7}$$

t, adimensional position of the minimum bending moment; x_{min}, position of the minimum bending moment with respect to point A.

In the following section the k and t ratios are estimated for different values of s, L and H.

3. Results

A parametric analysis of the $k = k(s, L, H)$ and $t = t(s, L, H)$ functions is carried out.

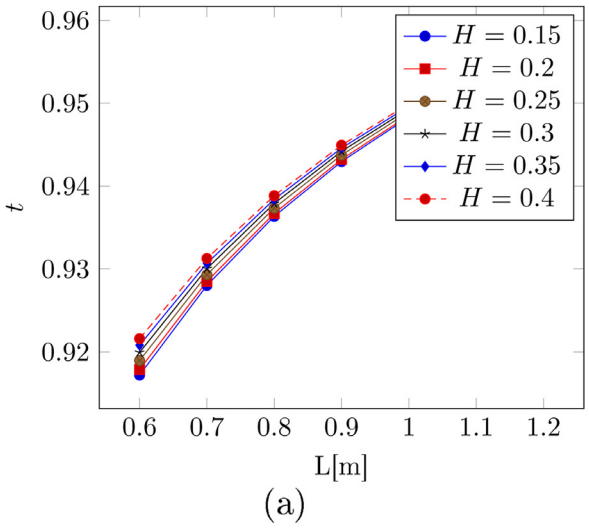

(a)

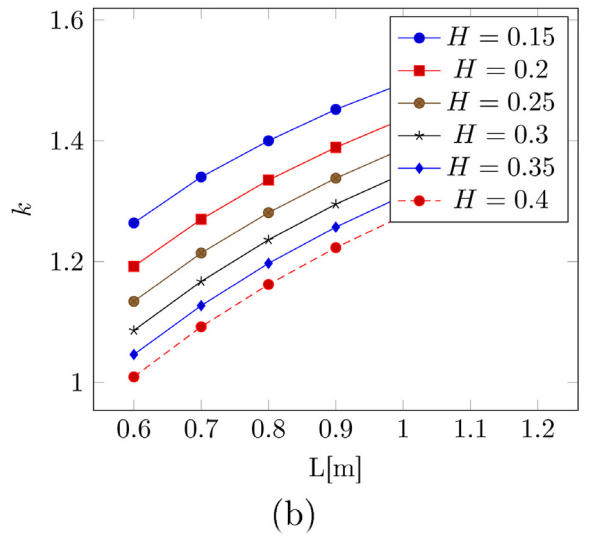

(b)

Fig. 8. Parametric analysis of the $t(L)$ (a) and $k(L)$ (b) functions for 6 different values of H, assuming $s = 1$ mm.

Assuming 3 different values of s (5 mm, 1 mm and 0.5 mm respectively), the $k = k(L)$ and $t = t(L)$ functions are plotted for 6 different values of H. In particular, Fig. 7 refers to $s = 5$ mm, Fig. 8 to $s = 1$ mm while Fig. 9 to $s = 0.5$ mm.

From Fig. 3–5, an increase in the elastic medium rigidity (c) does not sensibly affect x_{min} values, determining important excursions of the k factor.

For values of s sufficiently small and increasing values of L and H, the bending moment over the supports (M_{min}) is long greater than the corresponding M_{max} value.

In the curve in Fig. 9(b), although extorted for H and L values incompatible with the static safety of the architrave, the k factor reaches values greater than 1.5.

- Assuming the *Maximum Normal Stress Theory* [19] as Resistance Criterion, it is more likely that the architrave breaks over the supports rather than in the middle span, as c and L increase while H decreases. This may be evidenced by some broken architraves in Fig. 10.
- The position of the minimum bending moment (x_{min}) does not strongly depend on the three parameters s, L and H. It shows a modest increase, when c and L decrease and L increases ($t \in \{0.85 - 0.95\}$).

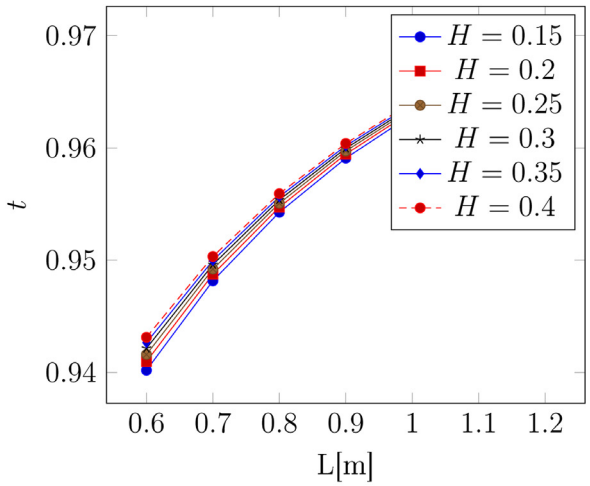

(a)

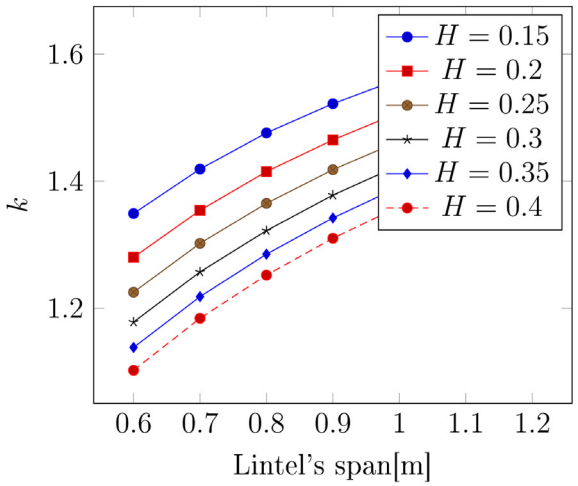

(b)

Fig. 9. Parametric analysis of the $t(L)$ (a) and $k(L)$ (b) functions for 6 different values of H, assuming $s = 0.5$ mm.

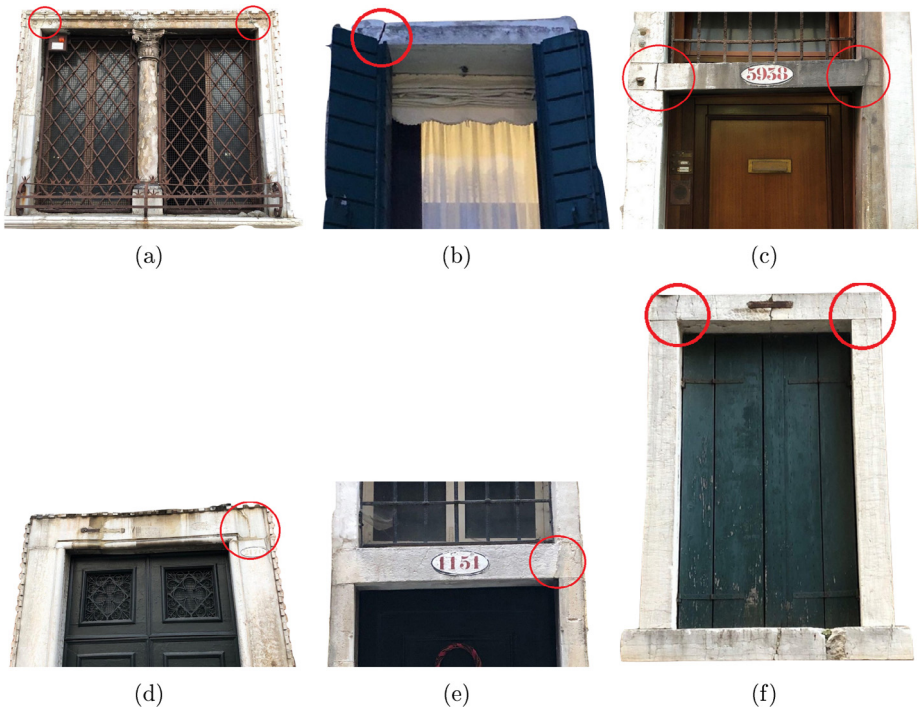

Fig. 10. Examples of monolithic architraves showing cracks over the supports.

In real stone architraves, many causes may concur to its cracking, even more to the crack localization.

For some values of c, L and H, if the uniform load p is large enough, it may be very likely, according to the proposed model, that the crack is located by the supports, rather than in the middle span of the beam.

4. Conclusions

Under particular geometric, constraint and loading conditions, it may be more likely that stone lintels will crack by the supports, rather than in the middle span.

This phenomenon surely does not endanger the statics of a building (vertical loads), nevertheless it may cause unsightly lesions, greatly reducing the due toothing of the architrave into the masonry for seismic safety purposes.

The observation of these cracks probably aroused the creativity of local masters determining the birth of the architrave *a tasselli*, the Piece-Type (PT) architrave: if a fracture is artificially made, if the architrave is disjointed into three portions (the mid block and the two pieces or *tasselli*), it is unlikely that the element will crack over the supports. The analytical model, presented in the current paper, roughly describes the behaviour of stone lintels, however it cannot be used to predict the best width of the *tassello*; The model does predict a crack close to the end of the support, by the opening, in monolithic architraves [19].

Understanding the roots of this technique makes us aware actors in the restoration process [20]: The PT architrave does not appear the product of the inattention of master builders, but the oral memory trace of a local construction tradition.

References

[1] C. Varagnoli, Tecniche costruttive tradizionali e terremoto, Ricerche di storia dell'arte 32 (3) (2009) 65-0.
[2] C. Varagnoli, et al., La costruzione tradizionale in Abruzzo: fonti materiali e tecniche costruttive dalla fine del Medioevo all'Ottocento, Gangemi Editore spa, 2011.
[3] G. Ameri, M. Massa, D. Bindi, E. D'Alema, A. Gorini, L. Luzi, S. Marzorati, F. Pacor, R. Paolucci, R. Puglia, et al., The 6 April 2009, mw 6.3, l'aquila (central Italy) earthquake: strong-motion observations, Seismol. Res. Lett. (2009).
[4] M. Baratta, I terremoti in Italia, vol. 6, Le Monnier, 1936.
[5] A. Ciccozzi, «where-it-was-as-it-was». the protection of cultural heritage and the seismic safety of buildings at l'aquila, Etnografia e ricerca qualitativa 8 (2) (2015) 259–276.
[6] S. Cecamore, La ricostruzione aquilana, antichi e nuovi presidi, ArcHistoR (4) (2015) 118–151.
[7] S. Cattari, S. Lagomarsino, A strength criterion for the flexural behaviour of spandrels in un-reinforced masonry walls, Proc. of 14th WCEE (2008).
[8] S. Lagomarsino, A. Penna, A. Galasco, S. Cattari, Tremuri program: an equivalent frame model for the nonlinear seismic analysis of masonry buildings, Eng. Struct. 56 (2013) 1787–1799.

[9] N. Gattesco, I. Clemente, L. Macorini, S. Noè, Experimental investigation on the behaviour of spandrels in ancient masonry buildings, Proc. of 14th WCEE (2008).
[10] G. Stockel, La città dell'aquila, Gallo Cedrone: L'Aquila, Italy.
[11] E. Valeri, L'Aquila: guida storico-artistica alla città e al territorio, Carsa, 2000.
[12] I.C. Gavini, Storia dell'architettura in Abruzzo, vol. 1, Studio bibliografico Adelmo Polla, 1983.
[13] S. Timoshenko, History of strength of materials: with a brief account of the history of theory of elasticity and theory of structures, Courier Corporation, 1983.
[14] R. Baldacci, Scienza delle costruzioni, Utet, 1983.
[15] S.P. Timoshenko, D.H. Young, Theory of Structures.
[16] E. Benvenuto, A. Becchi, M. Corradi, F. Foce, La scienza delle costruzioni e il suo sviluppo storico, Edizioni di storia e letteratura Rome, 2006.
[17] M. Hetényi, Beams on Elastic Foundation: Theory with Applications in the Fields of Civil and Mechanical Engineering, University of Michigan, 1971.
[18] R. Lancellotta, Geotechnical Engineering, CRC Press, 2014.
[19] F.P. Beer, R. Johnston, J. Dewolf, D. Mazurek, Mechanics of Materials, McGraw-Hill, 2006.
[20] J. Jokilehto, History of Architectural Conservation, Routledge, 2007.
[21] A. Aloisio, M. Fragiacomo, G. D'Alò, The 18th-century baraccato of l'aquila, Int. J. Arch. Herit. (2019) 1–15.